Journal of Southeast University (English Edition) Vol. 26, No. 3, pp. 426 – 430 Sept. 2010 ISSN 1003—7985

Analysis of secondary flow in shell-side channel of trisection helix heat exchangers

Wang Weihan Chen Yaping Cao Ruibing Shi Mingheng

(School of Energy and Environment, Southeast University, Nanjing 210096, China)

Abstract: The flow characteristics of shell-side fluid in the tube-and-shell heat exchangers with trisection helical baffles with 35° inclined angles are numerically analyzed. The secondary flow distribution of the fluid in the shell-side channel is focused on. The results on meridian planes indicate that in the shell-side channel, the center part of fluid has an outward tendency because of the centrifugal force, and the peripheral region fluid has an inward tendency under the centripetal force. So in a spiral cycle, the fluid is divided into the upper and lower beams of streamlines, at the same time the Dean vortices are formed near the left baffle, and then the fluid turns to centripetal flow near the right baffle. Finally the two beams of streamlines merge in the main flow. The results of a number of parallel slices between two parallel baffles with the same sector in a swirl cycle also show the existence of the secondary flow and some backward flows at the V-gaps of the adjacent baffles. The secondary flows have a positive effect on mixing fluid by promoting the momentum and mass exchange between fluid particles near the tube wall and in the main stream, and thus they will enhance the heat transfer of the helix heat exchanger.

Key words: trisection helix heat exchangers; secondary flow; Dean vortices; heat transfer enhancement; flow field analysis

Vortex flow used in the heat exchanger is a low-cost and high-efficiency passive technology of heat transfer enhancement, and it is applicable in both tube-side and shell-side[1]. The spiral plug flow fluid in the shell-side of helix heat exchanger is beneficial to eliminate the stagnant-zone, enhance the heat transfer, reduce the shell-side pressure drop, inhibit fouling and reduce the flow-induced tube vibration damage. However, as the manufacturing process of continuous helical baffles is complicated, there had been little application until Lutcha et al.[2] proposed the structure of quadrant sector baffles. In recent years, the helix heat exchangers have been given great attention by scholars in related fields and the heat exchanger industry at home and abroad[3-7]. On this basis, Chen[8] put forward the scheme of a trisection helical baffle heat exchanger, which is suitable for the most widely used scheme of the equilateral triangle tube layout for tube-and-shell heat exchangers, and, therefore, it might have better application prospects than the quadrant one. Li et al.[9] presented the experimental results of the heat transfer and pressure drop performances of trisection baffled helix heat exchangers with different inclined angles.

The numerical simulation has been widely used by many researchers as a powerful computational and experimental means for demonstrating the flow and thermal fields in a heat exchanger. Zhang et al.[10] numerically simulated the shell-side laminar flow and heat transfer features by applying the porous media and the distribution of resistance model. Xu et al.[11] used Fluent software for numerical simulation of the shell-side flow and heat transfer of helix heat exchanger, and the phenomenon of short circuits near the heat exchanger axis position was found. Wang et al.[12] and Lei et al.[13] respectively studied the characteristics of the flow and heat transfer in heat exchangers with a number of helical baffle structures such as quadrant sector baffles, quadrant overlapped sector baffles, quadrant ellipse baffles, as well as the continuous helical baffle.

We consider the above-mentioned features of the helix heat exchanger connected with the secondary flow in the shell-side helical channel from the viewpoint of fluid mechanics. The discrete baffles form the helical channel one after another, forcing the fluid to generate a spiral flow, which is a combined movement of compulsory rotation and axial flow. And the secondary flow is accompanied with the spiral flow. The secondary flow can generate swirls to strengthen mixing between the fluid particles and scour the fluid boundary layer and fouling layers, thus, it enhances the heat and mass transfer. The secondary flow mainly includes the Dean vortices and the Taylor vortices[14-15]. However, it is not found so far in the relative research on the influence of the secondary flow on heat transfer characteristics in the shell-side channel of a trisection helix heat exchanger.

1 Physical and Mathematical Models

1.1 Physical model

The structure of the trisection helix heat exchanger is shown in Fig. 1. The physical model for calculation is shown in Fig. 2 (The numbers represent the baffle sequential number). The model is in the Descartes rectangular coordi-

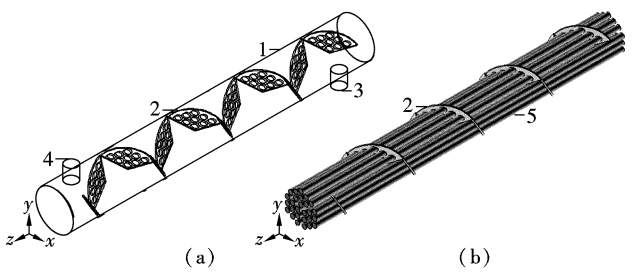

1—Shell; 2—Baffles; 3—Inlet; 4—Outlet; 5—Tube bundle

Fig. 1 Axonometric chart of trisection helix heat exchanger. (a) Shell and trisection helical baffles; (b) Trisection helical baffles and tubes

Received 2009-12-17.

Biographies: Wang Weihan (1981—), female, graduate; Chen Yaping (corresponding author), male, doctor, professor, ypgchen@sina.com.

Foundation items: The National Natural Science Foundation of China (No. 50976022), the National Key Technology R&D Program of China during the 11th Five-Year Plan Period (No. 2008BAJ12B02).

Citation: Wang Weihan, Chen Yaping, Cao Ruibing, et al. Analysis of secondary flow in shell-side channel of trisection helix heat exchangers[J]. Journal of Southeast University (English Edition), 2010, 26(3): 426 – 430.

nate, and the origin is the intersection point of shell centerline and inlet centerline. The heat exchanger has single shell and single tube bundle counter flow passages with an equilateral triangle tube layout. Tab. 1 lists the structure parameters of the heat exchanger and the baffles.

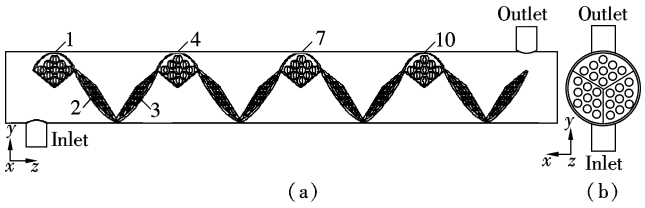

Fig. 2 Diagram of physical model of the trisection helix heat exchanger. (a) Main cutaway view; (b) Left cutaway view

Tab. 1 Structural parameters of the heat exchanger

Parameter	Value
Inner diameter of shell/mm	ϕ123
Outer diameter of tubes/mm	ϕ15
Number of tubes	27
Length of tube/mm	1 000
Tube layout	Equilateral triangle
Distance between centers of two adjacent tubes/mm	19
Inner diameter of inlet/outlet pipes/mm	ϕ40
Inclined angle of baffles/(°)	35
Pitch of baffles/mm	223.9
Number of baffles	12
Rotation direction of spiral	Right

1.2 Mathematical model

In order to simulate the secondary flow in the shell-side of the trisection helix heat exchanger, three-dimensional RNG turbulence models are applied. The governing equations for different variables can be expressed as follows[16]:

Continuity equation:

$$\frac{\partial u_i}{\partial x_i} = 0 \tag{1}$$

Momentum equation:

$$\frac{\partial}{\partial t}(\rho u_k) + \frac{\partial}{\partial x_i}(\rho u_i u_k) = \frac{\partial}{\partial x_i}\left(\mu \frac{\partial u_k}{\partial x_i}\right) - \frac{\partial P}{\partial x_k} \tag{2}$$

Energy equation:

$$\frac{\partial}{\partial t}(\rho T) + \frac{\partial}{\partial x_i}(\rho u_i T) = \frac{\partial}{\partial x_i}\left(\lambda c_P \frac{\partial T}{\partial x_i}\right) \tag{3}$$

The calculation is based on the following assumptions: 1) Constant properties; 2) Fully developed turbulent in the shell-side channel; 3) Ignoring viscous dissipation and mass force.

1.3 Boundary conditions

The boundary conditions are described as follows:

1) The shell inlet: $u = w = 0$, $v = 1.0$ m/s; $T_{in} = 353$ K(80 ℃);

2) The shell outlet: P_{out} is the pressure-outlet;

3) The heat exchanger tube wall surfaces: $u = v = w = 0$; $T_w = 283$ K (10 ℃) (constant);

4) The outer shell walls: $u = v = w = 0$; $\partial T/\partial n = 0$(thermal insulation walls);

5) The baffle walls: $u = v = w = 0$; $\partial T/\partial \boldsymbol{n} = 0$(thermal insulation walls), where u, v, w are velocities in different directions (m/s), and $\boldsymbol{n}$ is the normal vector of a plane.

1.4 Secondary flow parameters

The Dean number of the water flow in elbow pipe on the horizontal plane is defined as[14]

$$De = Re\sqrt{\frac{d_i}{d_c}} \tag{4}$$

where Re is the Reynolds number; d_i is the inner diameter of pipe, and d_c is the winding diameter of pipe.

For the shell-side channel of the helix heat exchanger, d_i is the distance between the outer ring of the tube bundle and the shell axis, and d_c is $\sqrt{2}/2$ of the inner diameter of the shell. Considering the pitch b, the effective winding diameter is

$$d'_c = d_c\sqrt{1 + \left(\frac{b}{\pi d_c}\right)^2} \tag{5}$$

1.5 Numerical method

The computations are carried out using FLUENT. For the complex three-dimensional model shown in Fig. 1, a hybrid mesh based on Pyramid/Wedge grid elements is applied. A non-uniform grid in the shell-side helical channel cross section is arranged with local grid refinement on both the shell-side wall and the tube wall to resolve fluid flow with consideration for the boundary layer flow effect. A grid independence test is conducted using several different mesh sizes for the trisection helix heat exchanger. This test proves that the results based on the grid system are independent of the mesh size and the validity of the numerical analysis can be ensured.

The numerical solutions of Eqs. (1) to (3) for the mass, velocity and pressure fields in the helical channel are obtained by means of the control volume finite-difference technique and the SIMPLE algorithm. The second-order upwind scheme is used for the numerical simulation. The solution is regarded as convergent not only by examining residual levels of velocity below 10 to 5, but also by monitoring relevant integrated quantities and checking the mass balances. The CPU time of computation for a typical case is about 24 h.

2 Results of Simulation

2.1 Whole flow field

The distribution of the shell-side streamlines in the trisection helix heat exchanger is obtained through simulation as shown in Fig. 3. The tubes are hidden to give a clearer figure. It can be seen that the shell-side fluid flows helically

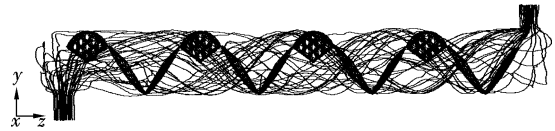

Fig. 3 Streamlines in the shell-side of trisection helix heat exchanger

under the guidance of 1/3 helical baffles, and there is hardly any stagnant zone in the shell-side channel.

2.2 Distribution of secondary flows

In the shell-side channel of the helical baffles heat exchanger, the streamline of the circumferential rotating fluid has outward tendency because of the centrifugal force. The centrifugal component of the flow can be demonstrated in a meridian plane. However, the outward flow results in a pressure gradient distribution that is higher in the periphery than in the center, and this forces centripetal flow toward the axis in the low-velocity region near the baffles wall. In this way, pairs of vortices rotating in the opposite direction will be formed. The schematic diagram of section locations with the secondary flows is shown in Fig. 4. In order to show the streamline in space without a tube barrier, the slices in Fig. 5, Fig. 6 and Fig. 7 are arranged at the intervals of the tube arrays. The schematic diagram of meridian plane locations is shown in Fig. 4(a). The shell walls are at the top of Fig. 5 and Fig. 6, and at the bottom of Fig. 7, respectively.

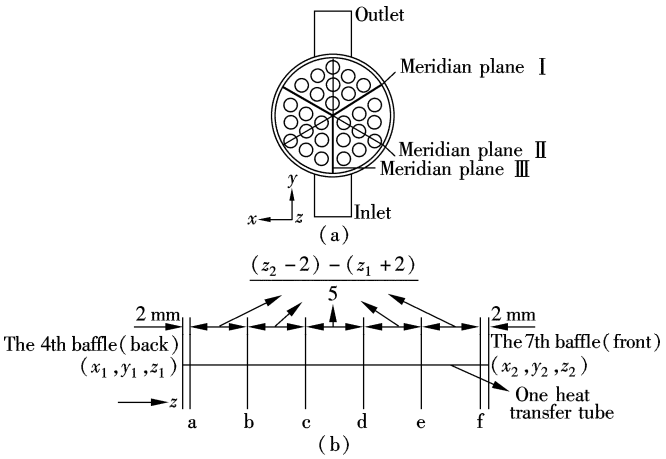

Fig. 4 Schematic diagram of section locations with the secondary flows. (a) Position of meridian planes; (b) Position of sections between the 4th and the 7th baffles

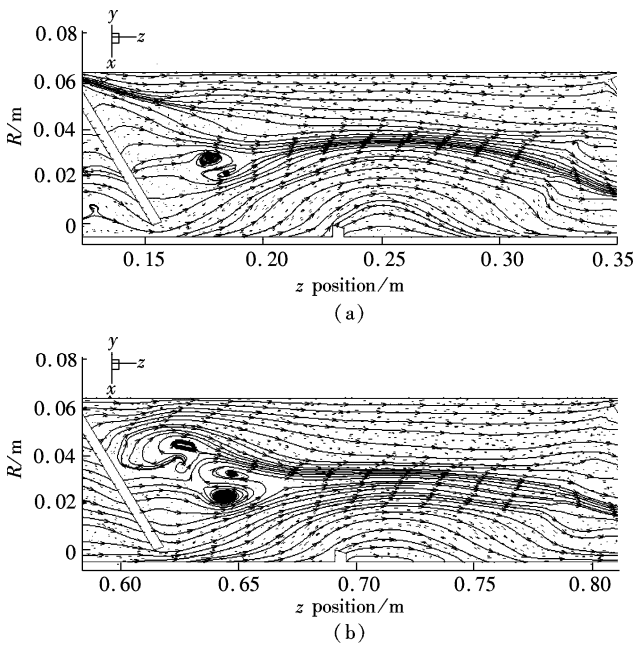

Fig. 5 Flow field on meridian plane I along axial z. (a) From 0.05 to 0.35 m; (b) From 0.58 to 0.82 m

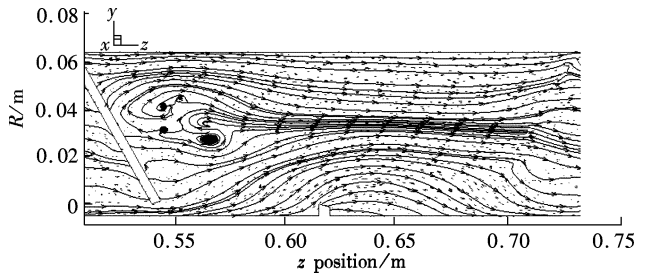

Fig. 6 Flow field on meridian plane Ⅱ along axial z from 0.51 to 0.74 m

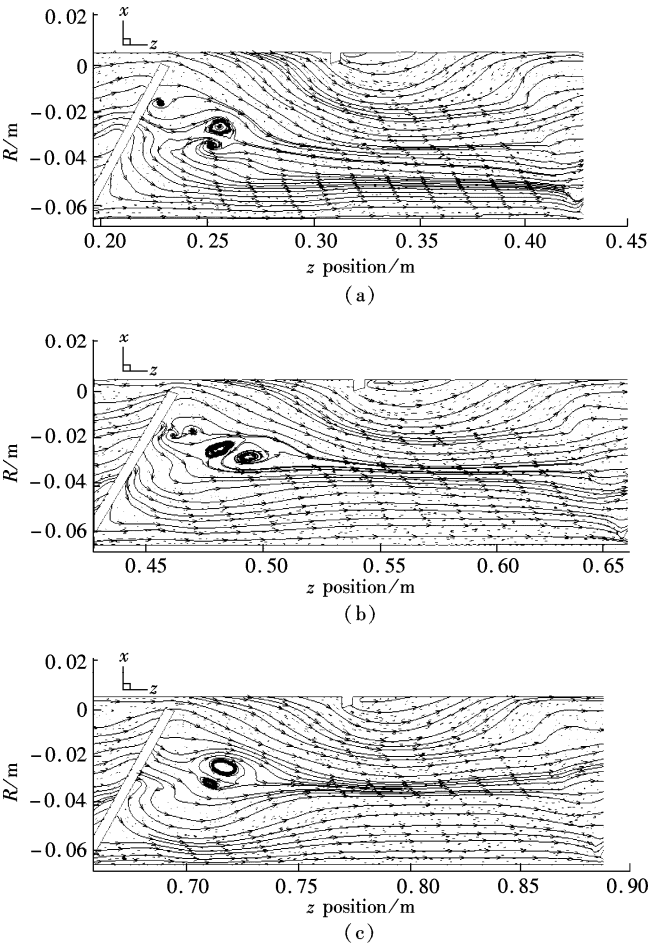

Fig. 7 Flow field on meridian plane Ⅲ along axial z. (a) From 0.20 to 0.43 m; (b) From 0.43 to 0.66 m; (c) From 0.66 to 0.88 m

It can be seen from Figs. 5, 6 and 7 that the flows in the helical baffle channel are quite complex, which not only can produce swirls, but also cause secondary flow. Ignoring the impact of the inlet and the outlet, in the shell-side channel of each spiral cycle, the shell-side fluid is divided into the upper and the lower streamlines with a distance of about 0.03 m from the axis. The fluid in the axial region expands toward the shell inner wall, while the fluid near the inner wall flows toward the axis. The above phenomenon proves that the centrifugal and centripetal forces coexist. Thus, at the position with a distance of about 0.04 m from the center of the left baffle and about ± 0.03 m from both sides of the axis along

each spiral cycle, it forms pairs of vortices rotating in the opposite directions—Dean vortex. Then, along the fluid flow direction, at the position with a distance of about 0.07 m from the center of the left baffle and about ± 0.03 m from both the sides of the axis, these two beams of streamlines begin to flow parallelly, which indicates that the shell-side fluid is balanced by the centrifugal force and the centripetal force at the moment. Finally, at the position with a distance of about 0.04 m from the center of the right baffle and about 0.02 m from the axis in the same spiral cycle, these two beams of streamlines begin to converge under the action of centripetal force, and at last are inhaled into the axial mainstream. Due to the complexity of the geometric structure of the flow channel in the trisection helix heat exchanger, it is obvious that the above-mentioned secondary flow does exist although it is not as typical as the binary vortices in a winding circular pipe. In some regions along the flow direction as shown in Figs. 5, 6 and 7, the vortices are prominent, and the flow is tied up by the vortex core, which can mix the fluid continuously, and thus the heat transfer is strengthened.

The distribution of the streamlines on the six parallel slices between the 4th and the 7th baffles, which are located in Fig. 4(b), are shown in Figs. 8(a) to (f). The incline angle and the magnitude of the slices are as the same as those of the baffles, to show the swirling flow movement in a swirl cycle between two baffles. Slice a is the streamline distribution closest to the back of the 4th baffle (+2 mm). We can see that along the shell-side channel, the fluid flows in a dextral direction, and the fluid densely gushes from the 4th baffle to slice a at the outer edge of the baffle and near the shell inner wall. But because of impact of the V-gap in the downstream of the 4th baffle, there is reverse flow toward the left inlet edge, while a vortex is formed at the right outlet edge and near the slice outer edge. When the fluid reaches slice b, the densely gushing streamlines at its outer edge begin to become gentle, and the reverse flow at the left inlet edge disappears. Because of the centrifugal force, the fluid begins to flow from the axis to the outer edge, and at the right outlet edge the vortex disappears at the moment, but the reverse flow deviating from the right outlet edge still exists. As for slice c, the fluid also flows from the axis to the outer edge under the action of centrifugal force, and we can see clearly that the above-mentioned location with reverse flow has become uniflow. To slice d and slice e, the streamline distribution is almost the same, the fluid gently flows from the inlet edge to the outlet edge, and the whole flow is normal. To slice f (The distance is −2 mm from the 7th baffle), the fluid has basically completed a spiral cycle flow in the shell-side channel. At the moment, we can see clearly that the fluid flows from the outer part of the inlet edge to the axis because of centripetal force, and the reverse flow appears again at its inlet edge just as in slice a. When the fluid leaves the outlet edge of slice f, it will enter the downstream channel formed by the 7th baffle and the 10th baffle to reform the vortex, and to start the next spiral cycle flow. Meanwhile, compared with Fig. 5, Fig. 6 and Fig. 7, we can see that the streamline distribution of the above six slices is well inosculated with the meridian plane in the same spiral cycle.

The phenomenon of reverse flow at the inlet edges of slice a and slice f, and at the outlet edge of slice b in Fig. 8 can be explained by the leakage flow at the V-gaps of adjacent baffle junction as shown in Fig. 9. As the baffles are plane, and the symmetry line of each baffle is perpendicular to the axis of the cylinder, while the inlet edge and the outlet edge are tilted in opposite directions, so the V-gap is formed by the adjacent baffles that touch at the periphery. Because the upstream compartment does not coincide with the downstream one, some fluid in the stage k compartment with lower static pressure will hold the velocity head to pass through the V-gap to the stage $k-1$ compartment with a higher static pressure. However, if the pressure difference of the adjacent compartments is greater than the local velocity head, the fluid flow in the upstream compartment of stage $k-1$ may reversely leak to stage k through the V-gap. The backward leakage flow problem does exist at the V-gaps. Some literature[5,7] suggested to apply axial overlap of the baffles to solve the problem, but Chen[8] pointed out that the axial overlap of the baffles can deteriorate the leakage problem, since it opens a bypass leakage channel to the downstream stage instead of the up-

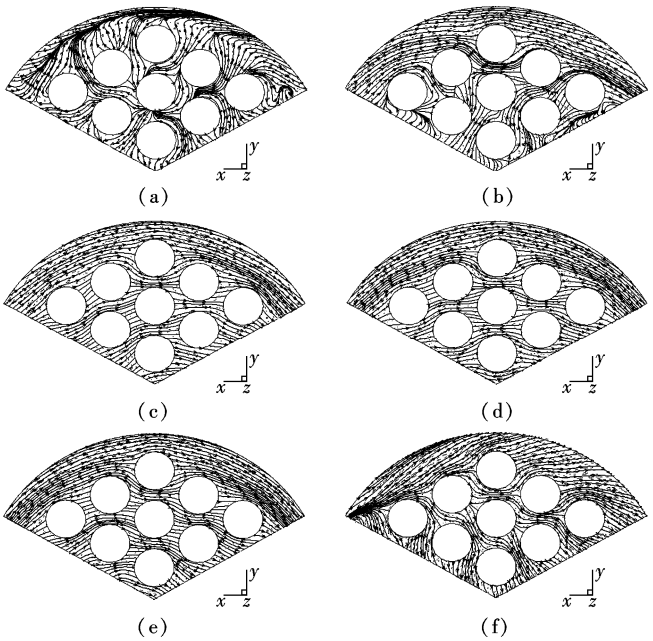

Fig. 8 Flow field on the parallel slices between the 4th and the 7th baffles. (a) Slice + 0.002 m from the 4th baffle; (b) Slice + 0.0447 m from slice a; (c) Slice + 0.0447 m from slice b; (d) Slice + 0.0447 m from slice c; (e) Slice + 0.0447m from slice d; (f) Slice − 0.002 m from the 7th baffle

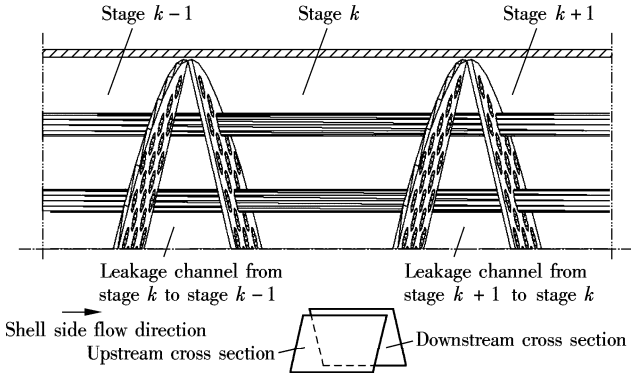

Fig. 9 Leakage flow through V-gaps of adjacent baffles

stream one. Song and Pei[7] introduced a circumferential overlap method for this issue, which seems reasonable.

3 Conclusions

1) The simulation results of streamlines on the three meridian planes clearly show that the Dean vortices secondary flow exists in the shell-side helical baffle channel of the trisection helix heat exchanger. The observed characteristics of the Dean vortices secondary flow show that the central part of the fluid has a trend of moving toward the periphery under the centrifugal forces, while the peripheral region of the fluid has a trend of moving toward the axis under the centripetal force, so a couple of the Dean vortices are formed near the baffle walls, and then the two beams of streamlines merge in the main flow.

2) The simulation results of streamlines on the multiple parallel slices between two parallel baffles with the same sector in a swirl cycle also show the existence of a vortex core source and the phenomenon of reverse leakage at the V-gaps at baffle junctions.

3) The secondary flow can mix the shell-side fluid continuously, and thus enhance the heat transfer.

References

[1] Gu Weizao, Shen Jiarui. *Heat transfer enhancement* [M]. Beijing: Science Press, 1990. (in Chinese)

[2] Lutcha J, Nemcansky J. Performance improvement of tubular heat exchangers by helical baffles [J]. *Chemical Engineering Research & Design*, 1990, **68**(3): 263 - 270.

[3] Stehlik P, Nemcansky J, Kral D, et al. Comparison of correction factors for shell-and-tube heat exchangers with segmental or helical baffles [J]. *Heat Transfer Engineering*, 1994, **15**(1): 55 - 65.

[4] Stehlik P, Wadekar V. Different strategies to improve industrial heat exchange [J]. *Heat Transfer Engineering*, 2002, **23**(6): 36 - 48.

[5] Andrews M, Master B I. Three-dimensional modeling of a helix changer heat exchanger using CFD [J]. *Heat Transfer Engineering*, 2005, **26**(6): 22 - 31.

[6] Master B I, Chunangad K S, Boxma A J, et al. Most frequently used heat exchangers from pioneering research to worldwide applications [J]. *Heat Transfer Engineering*, 2006, **27**(6): 4 - 11.

[7] Song Xiaoping, Pei Zhizhong. Shell and tube heat exchanger with anti-short circuit spiral baffle plate [J]. *Petro-Chemical Equipment Technology*, 2007, **28**(3): 13 - 17. (in Chinese)

[8] Chen Yaping. A novel helix baffled heat exchanger suitable for tube bundle arrangement with equilateral triangles [J]. *Petro-Chemical Equipment*, 2008, **37**(6): 1 - 5. (in Chinese)

[9] Li Yanqing, Chen Yaping, Liu Huajin, et al. Correlation equation of heat transfer coefficient at shell-side of trisection baffled helix heat exchangers [J]. *Journal of Southeast University*: *Natural Science Edition*, 2010, **40**(1): 149 - 153. (in Chinese)

[10] Zhang Jianfei, Li Xin, Wu Yang, et al. Numerical simulation of laminar and heat transfer in shell-and-tube heat exchanger with helical baffles [J]. *Journal of Engineering Thermophysics*, 2007, **28**(5): 853 - 855. (in Chinese)

[11] Xu Baiping, Wang Mingwei, Jiang Nan, et al. Numerical simulation study on the heat exchanger in the shell-side of the heat exchangers with helical baffles [J]. *Petroleum Processing and Petrochemicals*, 2005, **36**(10): 33 - 37. (in Chinese)

[12] Wang Chen, Sang Zhifu. Numerical study of shell-side flow of heat exchanger of different helical baffle [J]. *Petroleum Machinery*, 2008, **36**(10): 12 - 16. (in Chinese)

[13] Lei Yonggang, Chu Pan, He Yaling, et al. Numerical simulation of heat transfer and resistance characteristics of the restricted outgoing flow in a spiral channel [J]. *Engineering for Thermal Energy and Power*, 2007, **22**(6): 656 - 660. (in Chinese)

[14] Zhan Hanhui, Cheng Hao, Liu Jianwen, et al. *Secondary flow theory* [M]. Changsha: Central South University Press, 2006. (in Chinese)

[15] Kuakuvi D N, Moulin P, Charbit F. Dean vortices: a comparison of woven versus helical and straight hollow fiber membrane modules [J]. *Journal of Membrane Science*, 2000, **171**(1): 59 - 65.

[16] Shih T H, Liou W W, Shabbir A, et al. New eddy-viscosity model for high Reynolds number turbulent flows—model development and validation [J]. *Comput Fluids*, 1995, **24**(3): 227 - 238.

三分螺旋折流板换热器壳侧通道二次流分析

王伟晗 陈亚平 操瑞兵 施明恒

(东南大学能源与环境学院,南京 210096)

摘要:采用数值模拟方法分析了35°倾斜角三分螺旋折流板换热器壳侧流体流动特性,重点考察了壳侧通道的二次流分布.在子午切面上的结果表明:壳侧通道内轴心区域的流体受螺旋流动离心力的作用存在向外扩张的趋势,而外围区域的流体在向心力的作用下存在向轴心流动的趋势;在壳侧通道的每个螺旋周期内,流线分成上下2股,并在左侧折流板附近形成迪恩涡,在右侧折流板附近开始向心流动并最终被吸进轴向主流中.一个螺旋周期内平行的2块折流板之间多个平行切片的结果进一步证实了二次流的存在,同时还显示了V形缺口处存在的倒流现象.二次流有利于螺旋通道内流体的掺混,有效促进主流流体与近壁流体的动量和质量交换,从而可强化此类换热器的传热.

关键词:三分螺旋折流板换热器;二次流;迪恩涡;强化传热;流场分析

中图分类号:TK124